
Article:
Bonfiglio, P., Pompoli, F., Horoshenkov, K.V. et al. (1 more author) (2016) A simplified transfer matrix approach for the determination of the complex modulus of viscoelastic materials. Polymer Testing, 53. pp. 180-187. ISSN 0142-9418

https://doi.org/10.1016/j.polymertesting.2016.05.006

A SIMPLIFIED TRANSFER MATRIX APPROACH FOR THE DETERMINATION OF THE COMPLEX MODULUS OF VISCOELASTIC MATERIALS

Paolo Bonfiglio[1], Francesco Pompoli[1], Kirill V. Horoshenkov[2], Mahmud Iskandar B Seth A Rahim[2]

[1] Dipartimento di Ingegneria, Università degli Studi di Ferrara

Via Saragat 1, 44122 Ferrara, ITALY

[2] University of Sheffield, Department of Mechanical Engineering

Mappin Street, Sheffield, S1 1WB

Corresponding author

Paolo Bonfiglio

Dipartimento di Ingegneria, Università degli Studi di Ferrara, Via Saragat 1, 44122 Ferrara, ITALY

Tel.:+390532974876

paolo.bonfiglio@unife.it

Abstract

Nowadays several analytical and numerical approaches are available for analysing the performances of materials used in noise and vibration control applications. All these methodologies require knowledge of a set of input parameters which, in the case of viscoelastic materials, could exhibit strong dependence on the frequency in the entire audible range. The aim of this paper is to present a simplified transfer matrix approach for the determination of the complex modulus of isotropic viscoelastic materials as a function of frequency. To that effect, the tested material is excited by an electromagnetic shaker and longitudinal waves are investigated. Using a frequency sweep as an excitation signal, the time domain response is measured downstream and upstream of the sample itself. A velocity transfer function is measured and by using a transfer matrix model of the experimental setup, the complex wave number for longitudinal waves and consequently the complex modulus, once the Poisson's ratio is known in advance, can be determined. The results will be presented and discussed for different materials and compared with well-established quasi-static and dynamic techniques.

Keywords: viscoelastic materials, elastic properties, measurement methods

1. INTRODUCTION

In literature several quasi-static and dynamic methods have been proposed for determining mechanical properties of viscoelastic materials as a function of frequency. Jaouen et al. [1] presented and discussed a comprehensive review of existing methods for determining the mechanical properties of materials used in noise and vibration control applications. Recently Bonfiglio et al. [2] proposed a method for determining the values of the storage and loss moduli (hereafter indicated as E_1 [Pa] and E_2 [Pa]) in a wide frequency range measuring time domain accelerations and using a transfer matrix approach for wave propagations in linear homogeneous and isotropic elastic solids. The proposed methodology was applied at fixed frequencies in the range between 100 and 1500 Hz to open and closed cell viscoelastic materials and comparison with some of the methods described in ref. [1] was found to be consistent. Nevertheless the time domain method requires the use of a minimization based procedure for the determination of the complex modulus.

The aim of this paper is to extend the work presented in ref. [2] describing an analytic procedure for determining the complex modulus starting from an experimental test on materials in which only longitudinal waves are propagating.

Similarly to the methodology described in ref. [2] the entire measurement set-up is modelled using a transfer matrix procedure. Contrastingly, the set-up is simplified since no top plate is required during the tests and the determination of the complex modulus is direct because of the use of an analytical model for the measured velocity transfer function as described in following sections. In addition, the method allows for the narrow band measurement of the complex modulus in an extended frequency range.

A similar set-up was applied by Pritz [3] to closed-cell foam; in this case, the complex modulus is estimated at few frequencies from the analytical solution for only resonance frequencies and resonance magnitudes of the one-dimensional wave equation.

The paper is organised as follows. Section 2 reports the description of the methodology. A description of the experimental set-up, tested materials is given in Section 3. Section 4 will show results obtained using the proposed methodology and the comparison between different measurement techniques. Concluding remarks will be made in the last section.

2. DESCRIPTION OF THE METHODOLOGY

The measurement procedure is summarised as follows. The tested material (here assumed to be homogeneous and isotropic) is mounted on an aluminium support plate which is excited by an electromagnetic shaker. Using a logarithmic sine sweep as the excitation signal, the accelerometric response $a_{in}(t)$ [m/s^2] at the bottom plate is measured using an accelerometer and the velocity response $v_{out}(t)$ [m/s] at top surface of the sample is determined using a laser vibrometer, as shown in Fig. 1.

Assuming a time harmonic behaviour ($e^{i\omega t}$) of the measured quantities, from the experimental tests it is possible to calculate the velocity transfer function as follows:

$$H_{v,exp} = \frac{V_{in}(\omega)}{V_{out}(\omega)} = \frac{A_{in}(\omega)}{j \cdot \omega \cdot V_{out}(\omega)} \qquad [-] \tag{1}$$

where ω [rad/s] is the angular frequency and $A_{in}(\omega)$ [m/s^2] and $V_{out}(\omega)$[m/s] the complex frequency spectra calculated by applying a Fourier transform to acceleration and velocity in time domain, respectively.

In order to determine the complex modulus of a given material, the proposed methodology requires the measurement layout to be simulated using a well-established transfer matrix approach [4]. In fact, as fully described in ref. [2], it is possible to calculate in the frequency domain the complete set of vibro-acoustical indicators $\mathbf{V_2}$ (pressures, velocities, stresses) from the transfer matrix model for a given frequency and a semi-infinite fluid termination by solving the following expression:

$$[D_2]\mathbf{V_2} = F \tag{2}$$

$[D_2]$ being a square matrix obtained from a complete matrix D:

$$D = \begin{bmatrix} [I_{fs}] & [J_{fs}][T_s] & [0] \\ [0] & [I_{sf}] & [J_{sf}] \\ [0] & ... & -1 \quad \rho_0 c_0 \end{bmatrix} \tag{3}$$

when its second column is eliminated, and F represents the vector obtained by multiplying the eliminated second column by -1. In Eq. (3) ρ_0 and c_0 represent the air density and the sound speed, respectively.

From Eq.(2), fixing arbitrarily the amplitude of the bottom plate velocity to the unity,

it is possible to demonstrate that for a given frequency and at normal incidence the velocity transfer function is given as follows:

$$H_{v,TM} = \frac{1}{\mathbf{V}_2(N)} \quad [-] \tag{4}$$

N being the dimension of the squared matrix $[D_2]$.

In Eq. (3), $I_{fs,sf}$ and $J_{fs,sf}$ are the known coupling matrices between different layers and their exact expressions can be found in ref. [4] (pages 257-260), while matrix T_s refers to the tested material. In particular, T_s depends on material density ρ [kg/m^3], complex modulus $E=E_1+iE_2$ [Pa] and Poisson's ratio ν [-] of the material to be tested. If h indicates the thickness of the material, we can write:

$$T_s = \left[\Gamma(-h)\right] \cdot \left[\Gamma(0)\right]^{-1} \tag{5}$$

If we limit the analysis to normal incidence plane wave to the bottom plate, Γ(x) is equal to:

$$\Gamma(x) = \begin{bmatrix} 0 & 0 & i\omega\delta_3 \sin(\delta_3 x) & -\omega\delta_3 \cos(\delta_3 x) \\ -i\omega\delta_1 \sin(\delta_1 x) & \omega\delta_1 \cos(\delta_1 x) & 0 & 0 \\ -\omega^2\rho \cos(\delta_1 x) & i\omega^2\rho \sin(\delta_1 x) & 0 & 0 \\ 0 & 0 & \omega^2\rho \cos(\delta_3 x) & -i\omega^2\rho \sin(\delta_3 x) \end{bmatrix} \tag{6}$$

being:

$$\delta_1 = \sqrt{\frac{\omega^2\rho}{\lambda + 2\mu}} \quad \text{and} \quad \delta_3 = \sqrt{\frac{\omega^2\rho}{\mu}} \tag{7}$$

where λ and μ are respectively the first and second Lamè coefficients. Finally, Lamè coefficients are related to complex modulus and Poisson's ratio as follows:

$$\lambda = \frac{\nu \cdot E}{(1-2\nu)(1+\nu)} \text{ and } \mu = \frac{E}{2(1+\nu)} \tag{8}$$

Several authors have underlined that Poisson's ratio varies slowly with frequency and

is real-valued if the sample is analysed in a small deformation regime [5,6]; thus once this parameter has been calculated in advance (for example from a quasi-static test), it is possible to use the proposed methodology to determine the storage and loss moduli of the material. In effect, after simple manipulations we can write the following expression for the velocity transfer function:

$$H_{v,TM} = \cos\left(\tilde{k}_c h\right) + \frac{j\rho_0 c_0 \tilde{k}_c \sin\left(\tilde{k}_c h\right)}{\rho\omega} \quad [-] \quad (9)$$

when $\tilde{k}_c$ is the complex wave number:

$$\tilde{k}_c = \sqrt{\frac{\rho}{E}\frac{(2\nu-1)(\nu+1)}{(\nu-1)}} \quad \left[m^{-1}\right] \quad (10)$$

Equation (9) is formally identical to a plane wave propagation solution within rigid frame open cell porous materials [4]. A similar experimental approach can be used for measuring the characteristic impedance and the complex wave number of such materials once pressures and particle velocities have been measured at both sides of a sample mounted within an impedance tube [7,8]. As a direct result it is possible to measure a complex density and sound speed as a function of the frequency. The method used here makes the assumption that the effective density of the material is real-valued and independent of frequency and equals the density of the material itself. Finally, solving equation (9) in relation to the experimental velocity transfer function in Eq. (1) it is possible to calculate the complex wave number and consequently the complex modulus E. Unfortunately Eq. (9) is transcendental and the solution is not unique. Eq. (9) can be simplified assuming that the fluid (air) load effect of the air on the upper side of the material can be neglected (i.e. the longitudinal stress vanishes at the free end at high frequencies) leading to the following approximated expression for the velocity transfer function:

$$H_{v,TM,approx} = \cos\left(\tilde{k}_c h\right) \quad [-] \quad (11)$$

As a consequence, the complex wave number can be calculated from experimental

velocity transfer function as follows:

$$\tilde{k}_c = \frac{1}{h}\arccos\left(H_{v,exp}\right) \quad \left[m^{-1}\right] \qquad (12)$$

In order to verify the reliability of the approximation in Eq. (11), once $\tilde{k}_c$ has been calculated from experimental tests, Eqs. (9) and (11) can be plotted together to check their consistency in the entire frequency range of interest.
Finally if we pose:

$$k_m = \Re\left\{\tilde{k}_c\right\} \quad \text{and} \quad \eta_k = \frac{\Im\left\{\tilde{k}_c\right\}}{\Re\left\{\tilde{k}_c\right\}} \qquad (13)$$

it can be proved that:

$$E_1 = \frac{-n\rho\omega^2\left(\eta_k^2-1\right)}{k_m^2\left(\left(\eta_k^2-1\right)^2+4\eta_k^2\right)}\left[Pa\right] \quad \text{and} \quad E_2 = \frac{-2n\rho\omega^2\eta_k}{k_m^2\left(\left(\eta_k^2-1\right)^2+4\eta_k^2\right)}\left[Pa\right] \qquad (14)$$

with:

$$n = \frac{(2\nu-1)(\nu+1)}{(\nu-1)} \qquad (15)$$

Here it is worth mentioning that the arccos function in Eq. (12) is an analytic and multi-value function. In effect:

$$\begin{aligned}\arccos\left(H_{v,exp}\right) &= -j\cdot\ln\left(\lambda\right) = \\ &= -j\cdot\left\{\ln\left(|\lambda|\right)+j\cdot\left[\arg\left(\lambda\right)+2k\pi\right]\right\}\end{aligned} \qquad (16)$$

$$\text{with } k\in Z \quad \text{and } \lambda = H_{v,exp}+j\sqrt{1-H_{v,exp}^2}$$

The solution of Eq. (16) lies in the Riemann-surface S that covers the complex plane with k branches. The branch cuts of Eq. (16) are at $\Im\left\{H_{v,exp}\right\}=0$. So, if $\Im\left\{H_{v,exp}\right\}<0$

the correct solutions for the real and imaginary parts of Eq. (12) can be calculated as follows:

$$\begin{aligned} \Re\left\{\tilde{k}_c\right\} &= \frac{1}{h}\left(2\pi - \Re\left\{\arccos\left(H_{v,exp}\right)\right\}\right) \quad \left[m^{-1}\right] \\ \Im\left\{\tilde{k}_c\right\} &= -\frac{1}{h}\left|\Im\left\{\arccos\left(H_{v,exp}\right)\right\}\right| \quad \left[m^{-1}\right] \end{aligned} \tag{17}$$

Summarizing, once the Poisson's ratio is known in advance by measuring the downstream-upstream velocity transfer function across a test sample, it is possible to calculate its complex modulus using Eq. (14).

3. MEASUREMENT SET-UP AND TESTED MATERIALS

The experimental setup for measuring the top and bottom sample response consists of a Data Physics V4 electromagnetic shaker, a B&K Type 2716C power Amplifier, a PCB 352C22 accelerometer (sensitivity 9.65 mV/g and weight $1e^{-3}$ kg), a Polytec OFV 3001 laser vibrometer (sensitivity 5 mm/s/V), a PC equipped with an NI USB 4431 acquisition device and Labview® software for signal acquisition and post-processing.

Tests were carried out on the frequency range between 50 and 4000 Hz (step 6.4 Hz) and a logarithmic sweep of 10 s duration was used as an excitation signal.

A procedure was implemented during the tests to calibrate the entire system and minimise any uncertainties from the transfer function between accelerometer and laser vibrometer. In particular, removing the sample, a transfer function test was carried out in the frequency range of interest and in such conditions at each frequency of interest, it was possible to identify a correction transfer function which was applied to any successive test as shown in Fig. 2. In order to avoid lateral sliding of the materials during the tests, they were fixed to the bottom plates using a thin adhesive layer.

Experimental tests were carried out on three materials (polyurethane foam, reconstituted porous rubber and high density rubber) whose descriptions are summarized in Table 1. Each material was also tested by using a quasi-static method [9,10] (data given in Table 1) and the time domain method described in ref. [2]. Moreover a methodology based on the Time-Temperature Superposition principle, as described in ref. [11], was applied to materials A and C in the frequency range between 10 Hz and 10000 Hz and to material B from 10 Hz up to 1000 Hz.

4. RESULTS

Figure 3 shows the complex wave number for material A calculated either as a direct solution of Eq. (12) and Eq. (17). From the comparison it is observed a correct trend for both real and imaginary parts of the complex wavenumber at frequency higher than the first branch cut at around 2000 Hz. The application of Eq. (12) would lead to negative (meaningless) values of storage and loss moduli.

Figure 4 depicts the comparison between velocity transfer function calculated using Eqs. (9) and (11) for all the materials. From the figures it is possible to observe a satisfying approximation of Eq. (11).

Figures from 5 to 7 show the comparison in terms of storage and loss modulus between the proposed methodology and different methods for all the tested materials. From the figures is it possible to notice that the comparison between the different methods is consistent. In all the examined cases, a slight underestimation of the storage and complex moduli appears at frequencies lower than 100 Hz probably due to the approximation in Eq. (12). Calculating the mean value of storage and loss moduli between 50 and 100 Hz and comparing such values with quasi-static measurements, the percentage relative error is around 30 % for E_1 and 15 % for E_2.

In many practical applications (for example in design for vibration isolation) a key parameter to be measured is the force transmissibility function level [12] in frequency domain. Generally, the objective of vibration isolation is to reduce the transmitted force to the ground at acceptable values. Referring to set-up described in Fig. 8a such quantity can be defined as:

$$T = 20\log_{10}\left(\frac{F_2(\omega)}{F_1(\omega)}\right) \quad [\mathrm{dB}] \quad (18).$$

In such context it is important to use proper mechanical properties of the isolators as a function of frequency. A finite element approach was used for simulating the transmissibility function of tested materials when quasi-static complex modulus (from Table 1) and values from the proposed methodology (Figs. 5-7) are utilized. In order to estimate the transmissibility function level, an axial-symmetric finite element model was implemented (Fig 8b). Regarding the finite element model, a mapped mesh was used and the mesh size was created in accordance with the rule of six

elements per wavelength. The force at the bottom of the material was fixed at 1 N at each frequency and the transmitted force was evaluated as an average along the fixed constrained line (simulating the ground).

Comparison between transmissibility function calculated using quasi-static and dynamic complex modulus is shown in Fig. 9 for all tested materials. From the comparison it can be observed that the use of quasi-static complex modulus leads to a remarkable underestimation of the first resonance (where the highest fraction of force is transmitted) and of the damping of the entire system. The correct determination of resonance frequency and damping is crucial in practical isolation applications since they give a clear indication of the frequency range in which the isolator provides optimal performance.

4. CONCLUSIONS

This paper has presented and discussed a novel method for determining the values of the complex modulus as a function of the frequency of homogeneous and isotropic viscoelastic materials using a simplified transfer matrix approach. The results of the proposed methodology on open and closed cell materials were compared with data from well-established quasi-static and dynamic methods and the comparison can be considered satisfactory. Some discrepancies were observed at very low frequencies due to approximation of zero pressure load at the free end of the tested sample. Results from the proposed methodology can be utilized for correctly simulating and optimizing the performance of a viscoelastic material in real vibration or sound isolation applications.

REFERENCES

1. L. Jaouen, A. Renault, M. Deverge, Elastic and damping characterizations of acoustical porous materials: Available experimental methods and applications to a melamine foam, Applied Acoustics **69**–**12** 1129–1140 (2008).
2. P. Bonfiglio, F. Pompoli, Determination of the dynamic complex modulus of viscoelastic materials using a time domain approach, Polymer Testing 48 89-96 (2015).
3. T. Pritz, Transfer function method for investigating the complex modulus of acoustic materials: Rod-like specimen, Journal of Sound and Vibration, 81-3, 359–376 (1982).

4. J. F. Allard, N. Atalla, Propagation of sound in porous media, 1–354, John Wiley & Sons, United Kingdom (2009).

5. M. Giovagnoni, On the direct measurement of the dynamic Poisson's ratio. Mechanics of Materials 17, 33–46 (1994).

6. W. Warren and A. Kraynik, The linear elastic properties of opencell foams, J. Appl. Mech. 55, 341–346 (1988).

7. B.H. Song, J.S. Bolton, A transfer-matrix approach for estimating the characteristic impedance and wave numbers of limp and rigid porous materials, J. Acoust. Soc. Am. 107-3: 1131-1152(2000).

8. P. Bonfiglio, F. Pompoli. A single measurement approach for the determination of the normal incidence transmission, J. Acoust. Soc. Am. 124, 1577-1583 (2008).

9. E. Mariez, S. Sahraoui, J. F. Allard, Elastic constants of polyurethane foam's skeleton for the Biot model. In: Proceedings of Internoise pp 951–54 Liverpool, (1996).

10. P. Bonfiglio, F. Pompoli, P. Shravage, Quasi-static evaluation of mechanical properties of poroelastic materials: static and dynamic strain dependence and in vacuum tests, In: Proceeding of Acoustics 08 pp 29–34, Paris (2008).

11. M. Etchessahar, L. Benyahia, S. Sahraoui, J. F. Tassin, Frequency dependence of elastic properties of acoustics foams, J Acoust Soc Am **117** 1114–1121 (2005).

12. A. C. Nilsson, Vibroacoustics, TRITA-FKT 2000:15, pp 3-14, ISSN 1103-470X, Stockholm (2000).

Figure 1 –Measurement layout.

Figure 2 – Calibration procedure.

Figure 3. Complex wave number for material A. Comparison between solutions from Eqs. (12) and (17).

Figure 4 – Comparison between velocity transfer function calculated using Eqs. (9) and (11) for (a) material A, (b) material B and (c) material C.

Figure 5 – (a) Storage and (b) loss moduli for material A. Comparison between different methods.

Figure 6 – (a) Storage and (b) loss moduli for material B. Comparison between different methods.

Figure 7 – (a) Storage and (b) loss moduli for material C. Comparison between different methods.

Figure 8 – (a) Set-up for force transmissibility function level measurement. (b) Finite element model for force transmissibility function level simulations.

Figure 9 –Force transmissibility function level simulations using quasi-static and dynamic complex modulus. (a) Material A, (b) Material B and (c) Material C.

Table 1. Description of tested materials.

Material	**A**	**B**	**C**
Description	Reconstituted porous rubber (open cells)	High density rubber (open cells)	Polyurethane foam (closed cells)
Density [kg/m^3]	240	990	85
Thickness [mm]	25	38	26
Storage Modulus [Pa]	851203	2012760	141467
Loss Modulus [Pa]	357128	704466	51821
Poisson Ratio	0.09	0.12	0.18

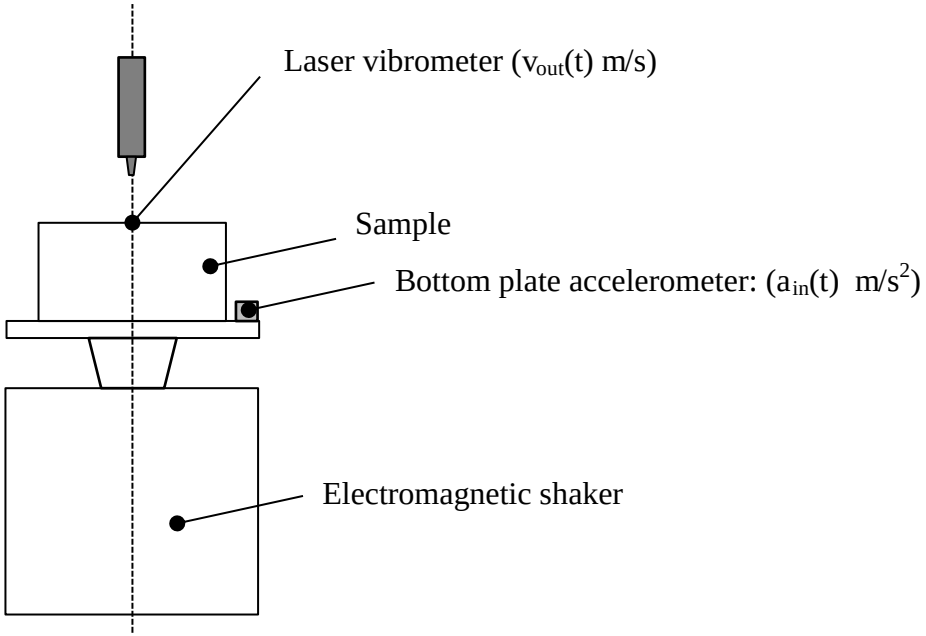
Laser vibrometer (v_{out}(t) m/s)
Sample
Bottom plate accelerometer: (a_{in}(t) m/s^2)
Electromagnetic shaker

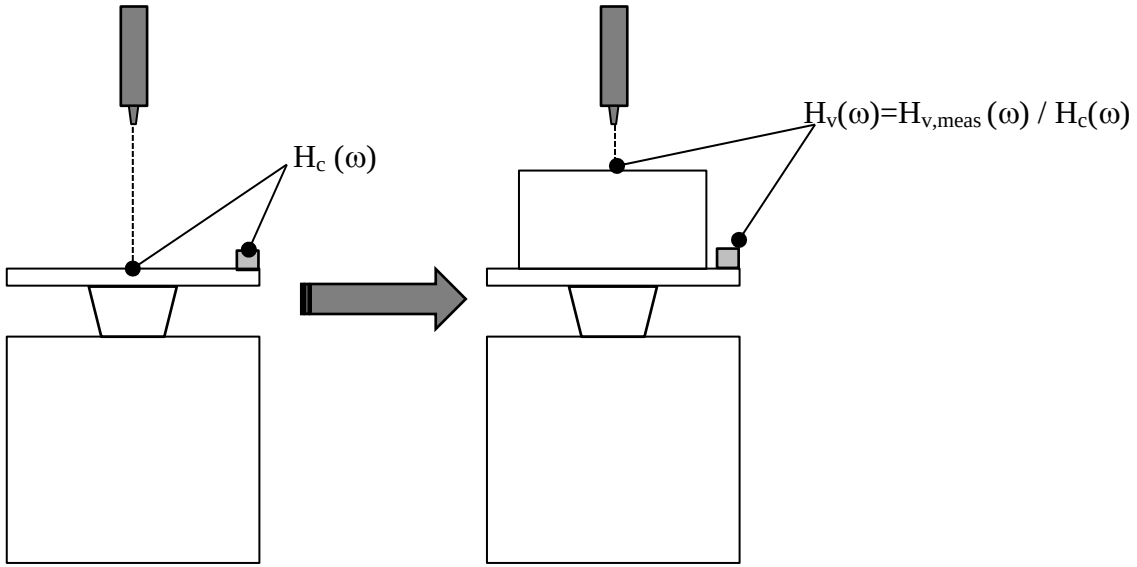
H_c (ω)
$H_v(\omega)=H_{v,meas}(\omega) / H_c(\omega)$

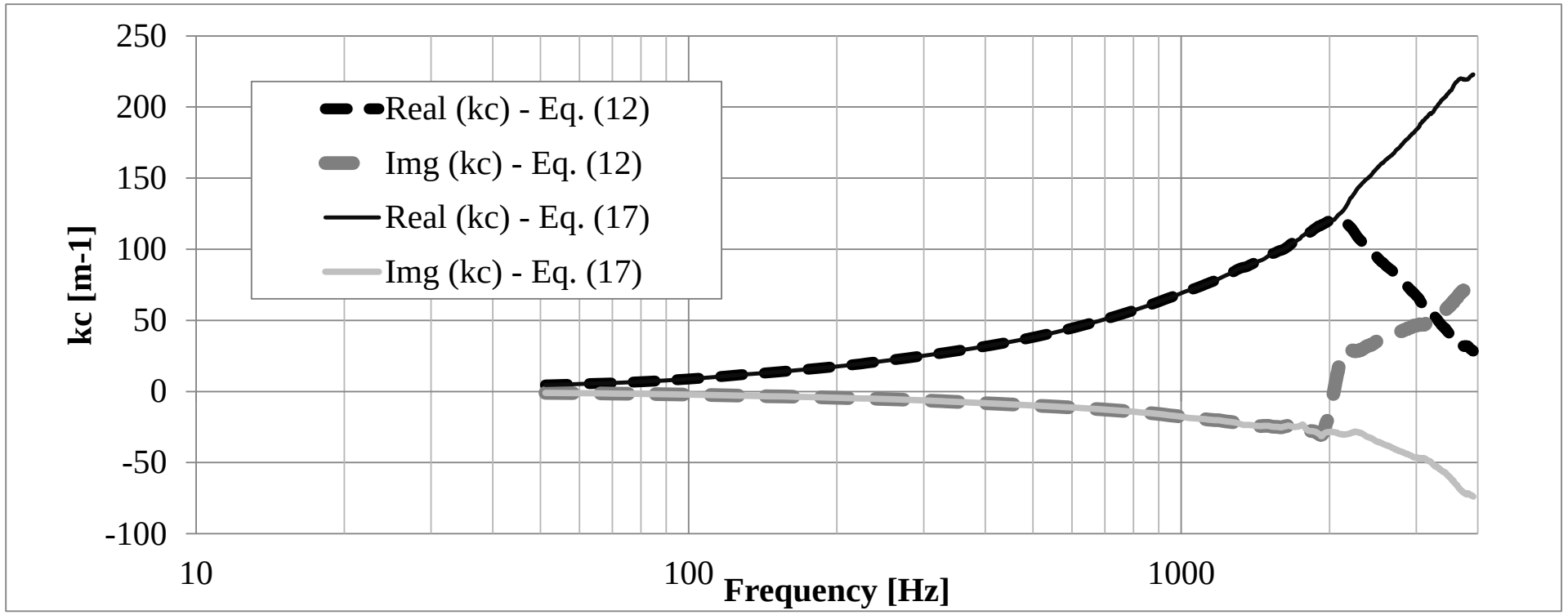
250
200
150
100
50
0
-50
-100
kc [m-1]
10
100
1000
Frequency [Hz]
Real (kc) - Eq. (12)
Img (kc) - Eq. (12)
Real (kc) - Eq. (17)
Img (kc) - Eq. (17)

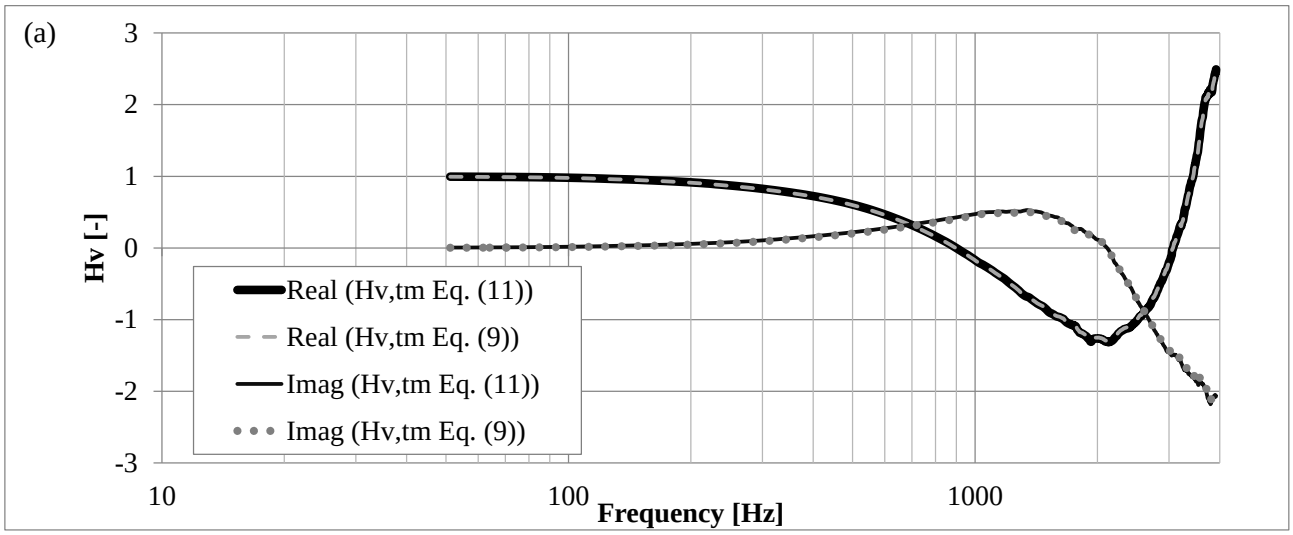
(a)
Hv [-]
Frequency [Hz]
Real (Hv,tm Eq. (11))
Real (Hv,tm Eq. (9))
Imag (Hv,tm Eq. (11))
Imag (Hv,tm Eq. (9))

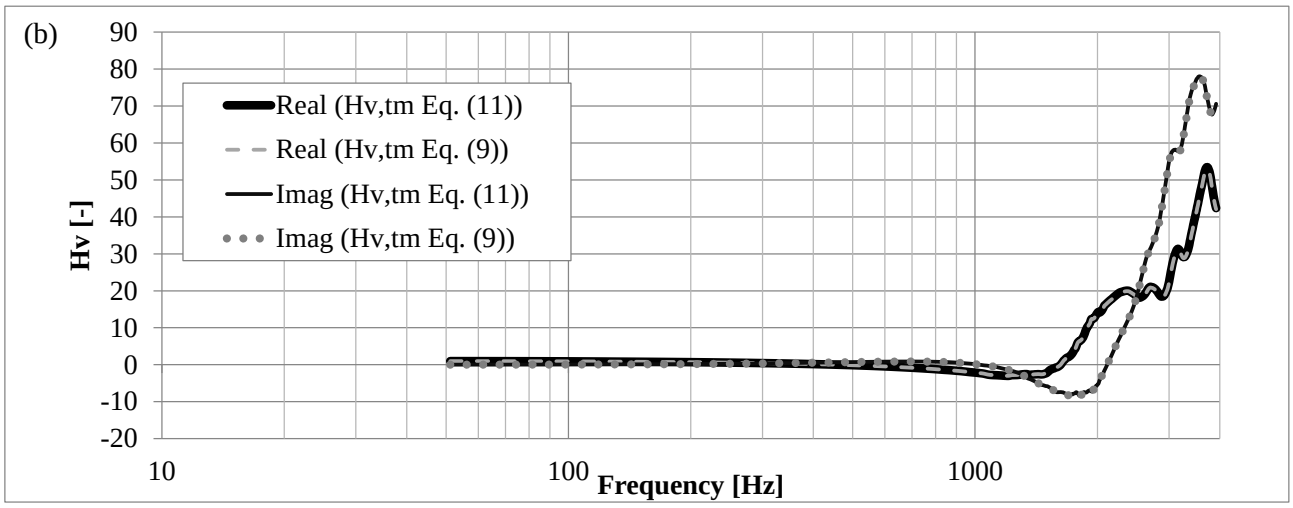
(b)
Hv [-]
Frequency [Hz]
Real (Hv,tm Eq. (11))
Real (Hv,tm Eq. (9))
Imag (Hv,tm Eq. (11))
Imag (Hv,tm Eq. (9))

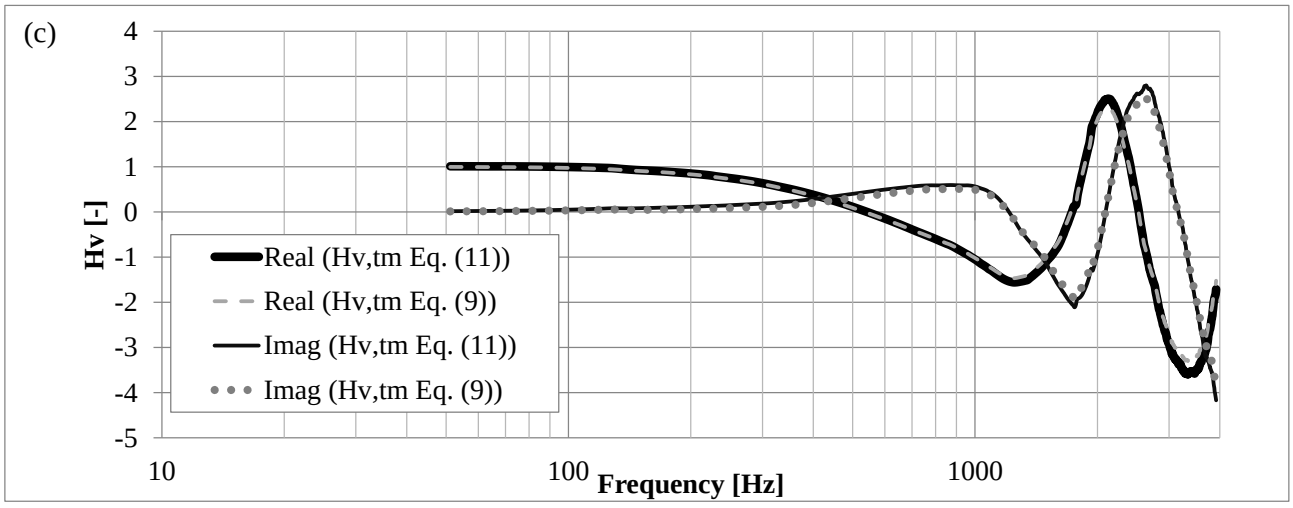
(c)
Hv [-]
Frequency [Hz]
Real (Hv,tm Eq. (11))
Real (Hv,tm Eq. (9))
Imag (Hv,tm Eq. (11))
Imag (Hv,tm Eq. (9))

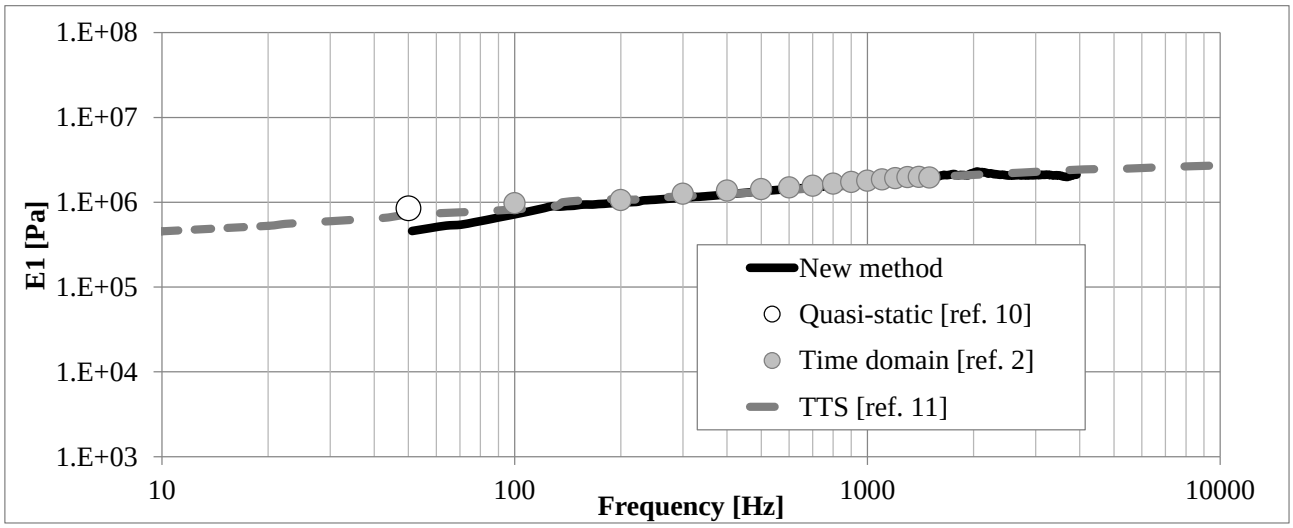
1.E+08
1.E+07
1.E+06
1.E+05
1.E+04
1.E+03
E1 [Pa]
10
100
1000
10000
Frequency [Hz]
New method
Quasi-static [ref. 10]
Time domain [ref. 2]
TTS [ref. 11]

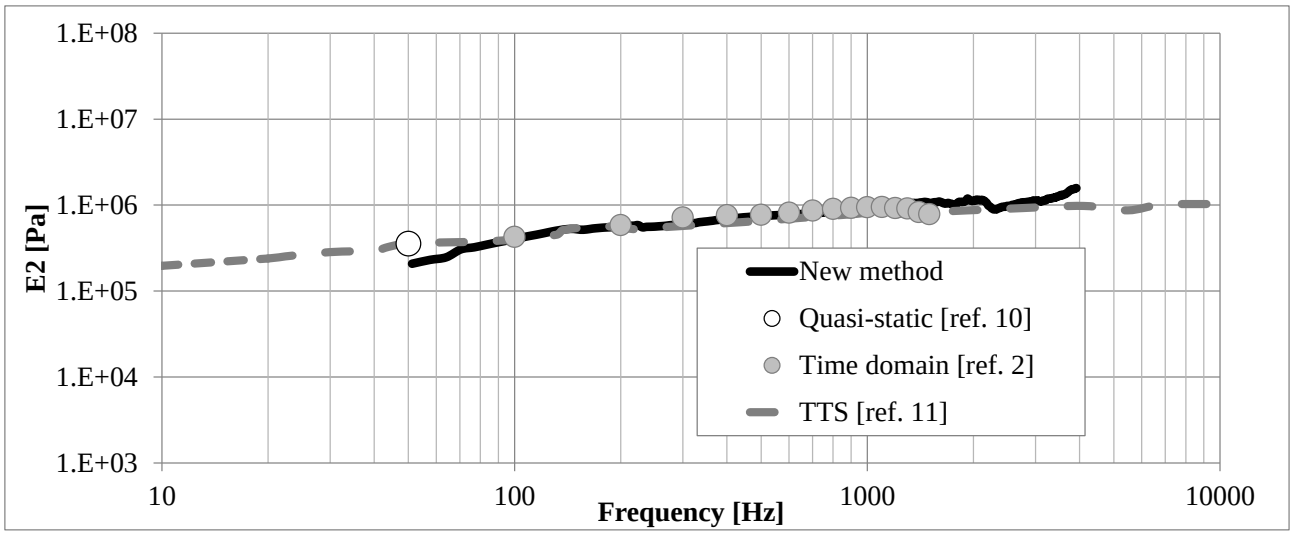
1.E+08
1.E+07
1.E+06
1.E+05
1.E+04
1.E+03
E2 [Pa]
10
100
1000
10000
Frequency [Hz]
New method
Quasi-static [ref. 10]
Time domain [ref. 2]
TTS [ref. 11]

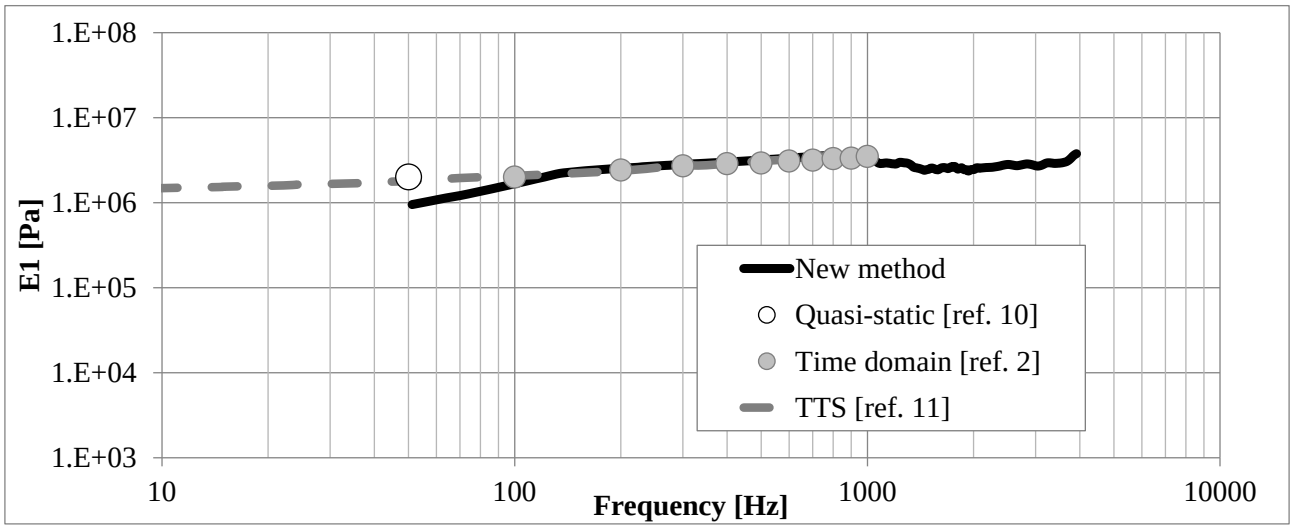
1.E+08
1.E+07
1.E+06
1.E+05
1.E+04
1.E+03
E1 [Pa]
10
100
1000
10000
Frequency [Hz]
New method
Quasi-static [ref. 10]
Time domain [ref. 2]
TTS [ref. 11]

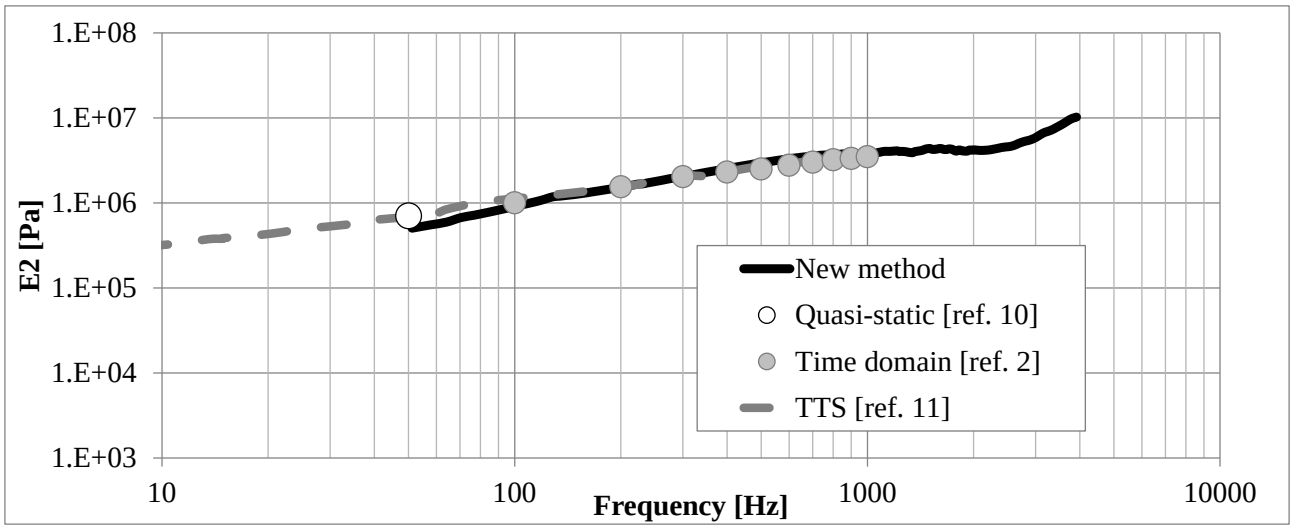
1.E+08
1.E+07
1.E+06
1.E+05
1.E+04
1.E+03
E2 [Pa]
10
100
1000
10000
Frequency [Hz]
New method
Quasi-static [ref. 10]
Time domain [ref. 2]
TTS [ref. 11]

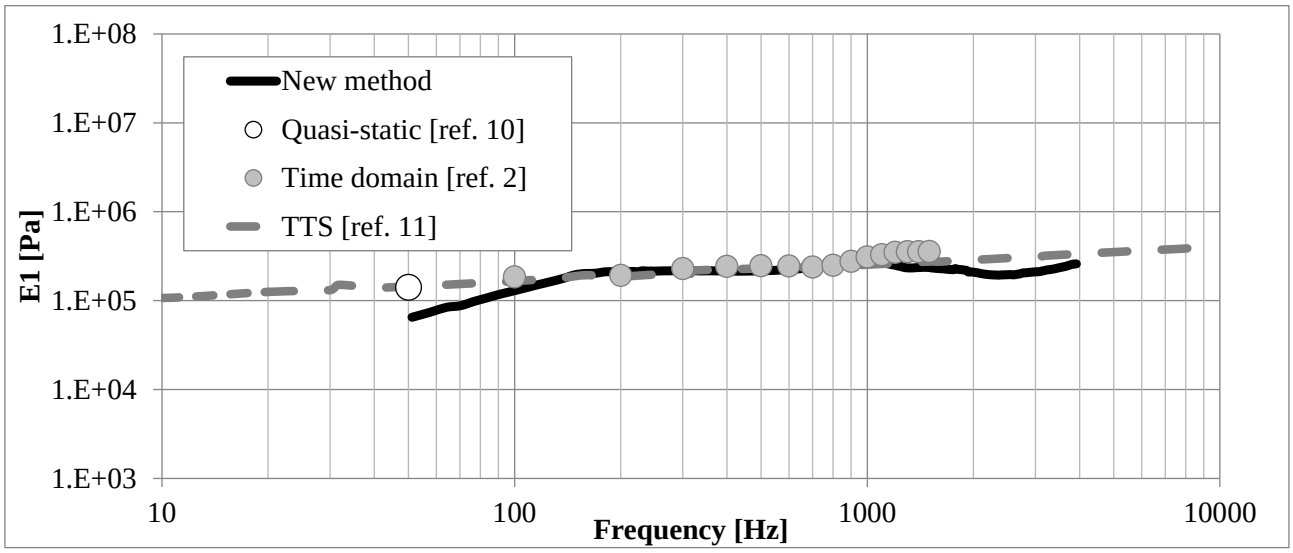
1.E+08
1.E+07
1.E+06
1.E+05
1.E+04
1.E+03
E1 [Pa]
New method
Quasi-static [ref. 10]
Time domain [ref. 2]
TTS [ref. 11]
10
100
1000
10000
Frequency [Hz]

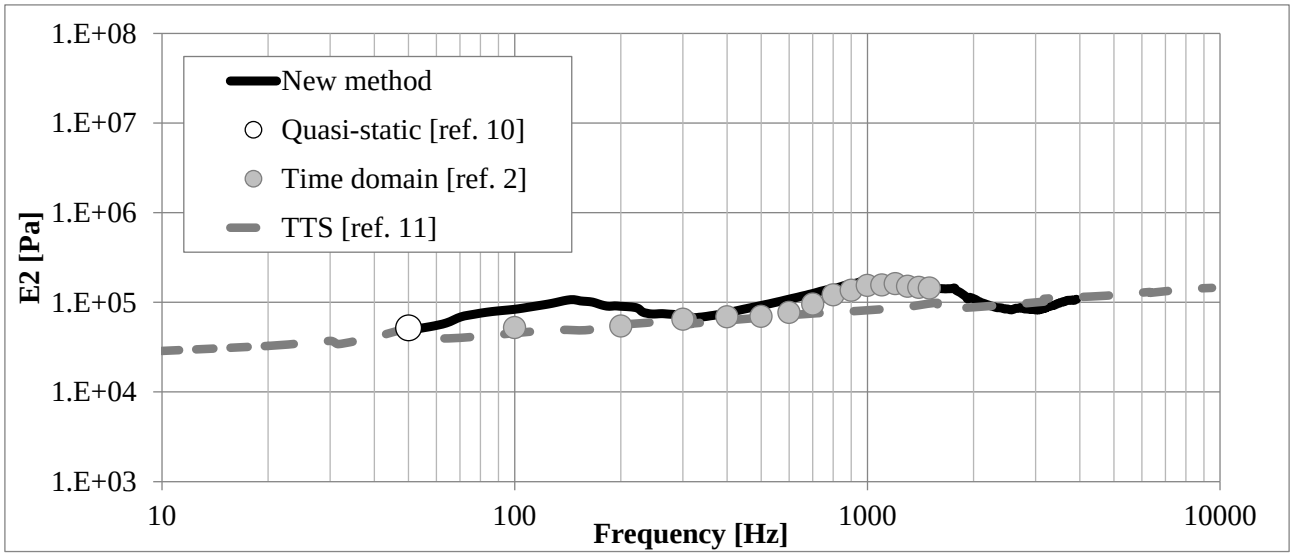
1.E+08
1.E+07
1.E+06
1.E+05
1.E+04
1.E+03
E2 [Pa]
New method
Quasi-static [ref. 10]
Time domain [ref. 2]
TTS [ref. 11]
10
100
1000
10000
Frequency [Hz]

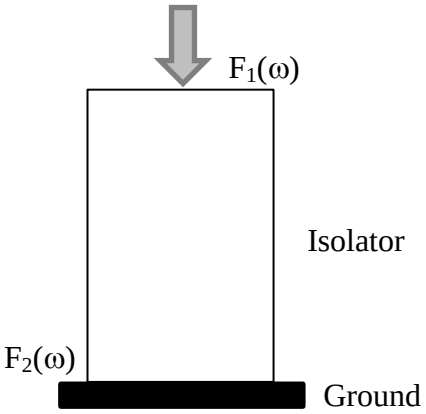
F1(ω)
Isolator
F2(ω)
Ground

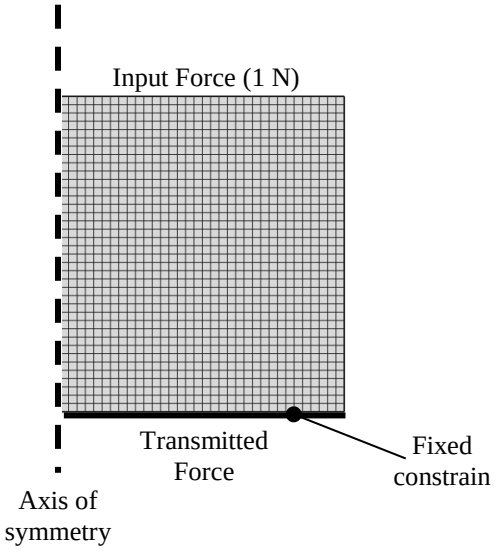
Input Force (1 N)
Transmitted Force
Fixed constrain
Axis of symmetry

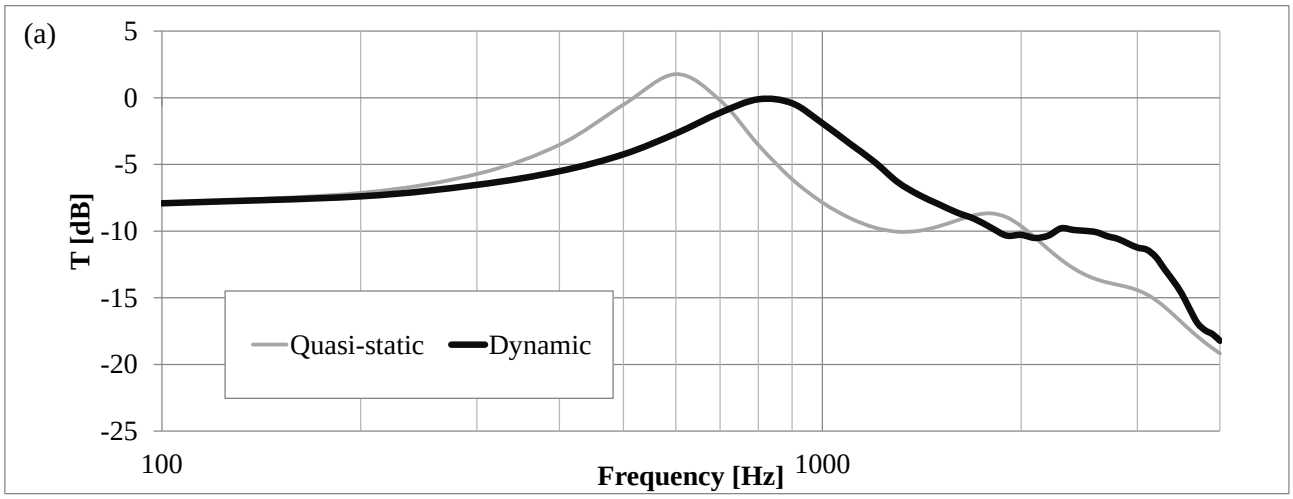
(a)
5
0
-5
-10
-15
-20
-25
T [dB]
Quasi-static
Dynamic
100
1000
Frequency [Hz]

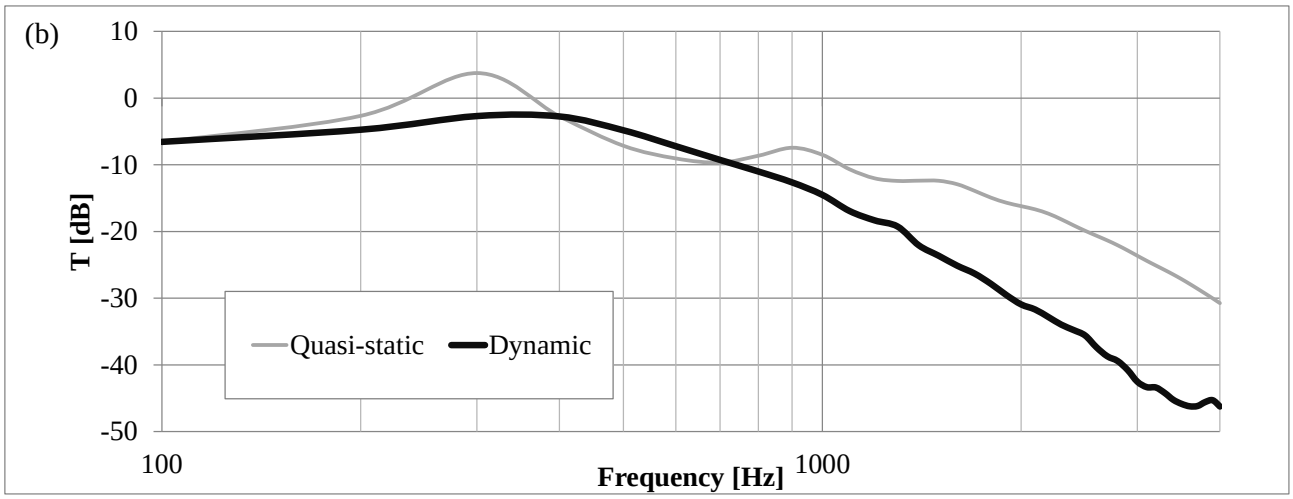
(b)
10
0
-10
-20
-30
-40
-50
T [dB]
Quasi-static
Dynamic
100
1000
Frequency [Hz]

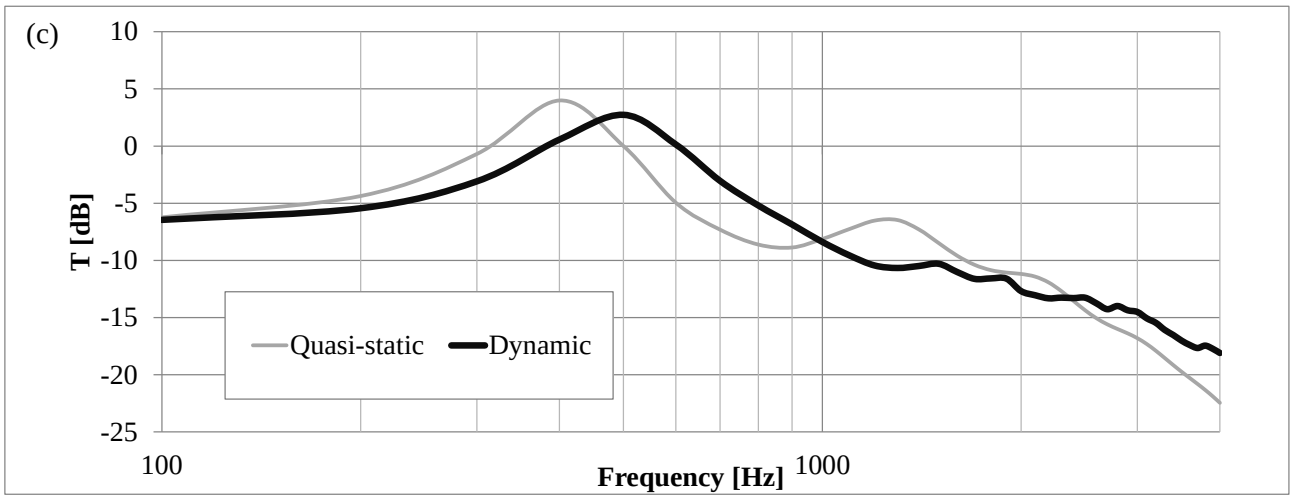
(c)
10
5
0
-5
-10
-15
-20
-25
T [dB]
Quasi-static
Dynamic
100
1000
Frequency [Hz]